ACS APPLIED MATERIALS & INTERFACES

Research Article

www.acsami.org

Osteogenic Differentiation Evaluation of an Engineered Extracellular Matrix Based Tissue Sheet for Potential Periosteum Replacement

Qi Xing, Zichen Qian, Baratwaaj Kannan, Mitchell Tahtinen, and Feng Zhao*

Department of Biomedical Engineering, Michigan Technological University, 1400 Townsend Drive, Houghton, Michigan 49931, United States

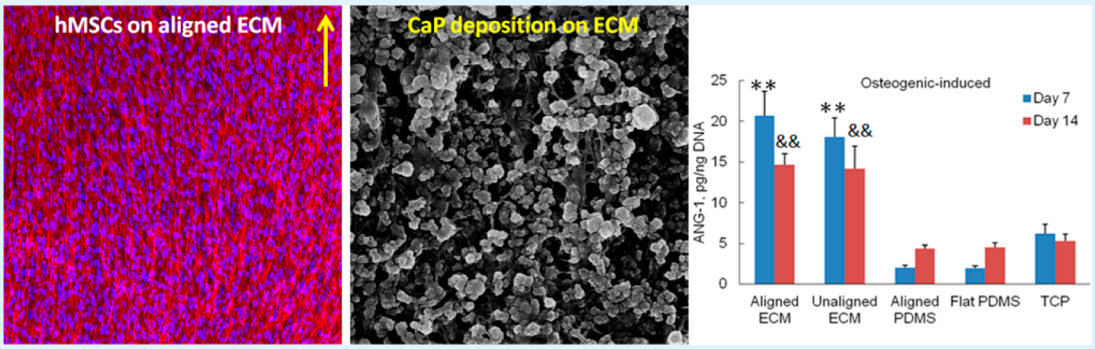

ABSTRACT: Due to the indispensable role of periosteum in bone defect healing and regeneration, a promising method to enhance osteogenesis of bone grafts by using an engineered biomimetic periosteum would be highly beneficial. The stromal microenvironment of periosteum is composed of various highly organized extracellular matrix (ECM) fibers, so an aligned natural ECM sheet, derived from the human dermal fibroblast cell sheet, may be advantageous when applied for artificial periosteum fabrication. Human mesenchymal stem cells (hMSCs) have been used to replace the osteoprogenitor cell population in native periosteum due to hMSCs' great osteogenic potential and fast in vitro expansion capacity. The objective of this work is to investigate if the natural ECM sheet and the substrate alignment can promote in vitro osteogenesis of hMSCs. The conventional cell culture substrates collagen I-coated polydimethylsiloxane (PDMS) and tissue culture plastic (TCP) were used as controls. It was found that the ECM sheet significantly increased alkaline phosphatase activity and calcium deposition. The enhanced osteogenic potential was further confirmed by increased bone-specific gene expression. The ECM sheet can bind significantly higher amounts of growth factors including ANG-1, TGF-β1, bFGF, and VEGF, as well as calcium phosphate nanoparticles, which contributed to high osteogenesis of the hMSCs on ECM sheet. However, the alignment of the substrates did not show significant influence on osteogenic activity and growth factor binding. These results demonstrated the great potential of hMSC-seeded ECM sheet as a biomimetic periosteum to improve critical sized bone regeneration.

KEYWORDS: *extracellular matrix sheet, mesenchymal stem cells, aligned substrate, osteogenic differentiation, biomimetic periosteum*

INTRODUCTION

The most commonly used bone grafts for treatment of critical sized bone defects are decellularized bone allografts.[1] Compared to engineered hard tissue scaffold such as bone cement, an allograft has excellent mechanical strength and fracture resistance. However, the healing and remodeling of an allograft is quite limited due to the lack of viable osteogenic and angiogenic cells.[2] Bone decellularization procedures remove the periosteum, which could result in over 60% decrease of new bone formation.[3] Periosteum is a membrane that covers outer surface of all bones. It consists of two distinct layers: the outer layer contains collagen fibers, fibroblasts, and microvessels; the inner layer contains osteoprogenitor cells that contribute to normal bone growth, healing, and remodeling.[4] It has been widely recognized that periosteum has remarkable regenerative capacity and plays an essential role in bone graft healing and remodeling.[5] Thus, a biomimetic periosteum covering an allograft surface may provide similar healing response.

The outer fibrous layer of native periosteum is predominantly composed of collagenous matrix interspersed with elastic fibers and fibroblasts.[4] Histology studies also revealed that the fibers are axially aligned suggesting the anisotropic structure of periosteum.[6] We have previously derived a natural extracellular matrix (ECM) sheet, from human dermal fibroblast cell sheet, which possesses a nanofibrous structure with abundant collagen and elastin fibers.[7] The fiber diameter is around 80 nm, similar to the size of collagen nanofibers found in native bones.[8] In addition, an aligned ECM sheet can be fabricated using a nanograted substrate to simulate the organized collagen fiber arrays present in native bones. The aligned ECM sheet has superior in vitro immunoregulatory properties compared to unaligned ECM.[7] Besides their similar collagenous composition and

Received: August 10, 2015
Accepted: September 29, 2015
Published: September 29, 2015

DOI: 10.1021/acsami.5b07386
ACS Appl. Mater. Interfaces 2015, 7, 23239−23247

structure to periosteum, ECM sheet contains other proteins and proteoglycans which are present in native periosteum.[9] Several studies have shown that cell-derived ECM can provide an osteogenic-inductive environment for bone regeneration. ECM synthesized by undifferentiated mesenchymal stem cells (MSCs) in vitro on plastic flasks has been shown to facilitate cell proliferation and enhance the osteogenic capacity of freshly reseeded MSCs.[10] Titanium fiber meshes decorated with rat bone marrow stromal cells significantly improved the deposition of mineralized matrix by MSCs.[11] Incorporation of MSC-derived ECM on polyurethane foams greatly upregulated mRNA expression of typical osteoblastic genes.[12] Besides ECM derived from MSCs, fibroblast-derived matrix, preosteoblast and endothelial cell-derived matrix were also found effective in increasing osteogenic marker expression.[13,14]

The inner layer of periosteum is mainly composed of osteoprogenitor cells. MSC is one type of osteoprogenitor cell that has been extensively studied in bone tissue engineering. MSCs can be easily harvested from various tissues such as bone marrow, adipose tissue, and skin. They have the ability to differentiate into multiple cell lineages including osteoblasts, adipocytes, and chondrocytes under their respective inductive environment.[15] In addition, MSCs can secrete a large amount of trophic factors, such as vascular endothelial growth factors (VEGF), transforming growth factor beta (TGF-β), and stromal cell derived factor-1 (SDF-1), to facilitate tissue regeneration.[16] Furthermore, MSCs have low immunogenicity and can be extensively expanded in vitro.[17] These superior properties make MSCs an excellent cell source for tissue regeneration, especially for bone repair. Most studies have chosen MSCs to construct engineered periosteum. A biomimetic periosteum composed of prevascularized and premineralized MSC sheets were wrapped around a biodegradable macroporous beta-tricalcium phosphate (β-TCP) scaffold to improve vascularization.[18] Polyethylene glycol-based hydrogels seeded with 50:50 MSCs and osteoprogenitor cells were used as periosteum to successfully improve allogenic bone graft healing in vivo.[19] Another study applied osteo-induced, MSCs-seeded, small intestinal submucosa (SIS) for allograft implantation to treat segmental bone defect.[20] However, these engineered periosteum still had different problems such as long preparation time, limited vascularization, and cell penetration ability. A biomimetic tissue-engineered periosteum with similar structure and function to native periosteum is desired for more efficient bone regeneration. The cellular construct consisting of MSCs and fibroblast-derived ECM sheet may serve the purpose.

The objective of the present work is to evaluate the in vitro osteogenic potential of human MSCs (hMSCs) cultured on an ECM sheet compared to other conventional substrates. A tissue engineered periosteum, mimicking the native bone alignment, may benefit the bone repair and remodeling process. Thus, the influence of alignment of the substrates was also considered. The cell growth and organization on different substrates were characterized. Osteogenic properties of hMSCs including alkaline phosphatase activity, ECM mineralization, and gene expression were compared in different cultures. The osteogenesis-related growth factors and calcium present in the microenvironment were analyzed to help understand the underlying mechanism.

MATERIALS AND METHODS

Production of Fibroblast Cell Sheet-Derived ECM. Polydimethylsiloxane (PDMS) substrates with (aligned) and without nanopattern (flat) (the gratings were 130 nm in depth and 350 nm in width) were coated with bovine collagen I to facilitate cell adhesion, following our previous publication.[21] Human dermal fibroblasts (ATCC, Manasass, VA) between passages 3 and 5 were seeded on the PDMS at a density of 10 000 cells/cm^2. The cells were cultured in Dulbecco's modified Eagle's medium (DMEM) supplemented with 20% fetal bovine serum (FBS), 20% Ham F12, 500 μM sodium ascorbate, and 1% penicillin/streptomycin (Life Technologies, Rockville, MD). The culture was maintained by changing medium twice per week and cells were allowed to proliferate for 6 weeks. The fibroblast cell sheet was decellularized following our previous publication.[7] Briefly, samples were placed into the first decellularization solution, which contained 1 M NaCl, 10 mM Tris, and 5 mM EDTA (Sigma, St Louis, MO). The cell sheet was shaken for 1 h at room temperature and rinsed thoroughly with phosphate buffered saline (PBS). The cell sheet was then placed in a second decellularization solution containing 0.5% SDS, 10 mM Tris, and 5 mM EDTA (Sigma), and shaken for 0.5 h at room temperature. After PBS wash, the sample was rinsed in DMEM medium with 20% FBS for 48 h at room temperature and rinsed again with PBS.

hMSCs Culture and Differentiation. Bone marrow-derived hMSCs were provided by Texas A&M University Health Sciences Center. The hMSCs were obtained following a method reported in our previous publication.[21] Briefly, bone marrow aspirates of about 2 mL were drawn from healthy donors ranging in age from 19 to 49 years under an Institutional Review Board approved protocol. Plastic adherent nucleated cells were separated from the aspirate and cultured as previously described. The decellularized ECM sheet (aligned and unaligned) were sterilized with 70% ethanol and rinsed with PBS. Passage 5 hMSCs were seeded on the ECM at the density of 5000 cells/cm^2 and cultured in complete culture medium (CCM) containing alpha-MEM supplemented with 20% FBS, 1% L-glutamine, and 1% penicillin/streptomycin (Life Technologies). Cells were also seeded on collagen I coated PDMS (aligned and flat) and tissue culture plastic (TCP) for comparison. At day 7 and day 14 samples were fixed, the F-actin was stained with rodamine phalloidin, and DAPI. The immunofluorescence staining was viewed by Olympus Fluoview FV-1000 confocal fluorescence microscopy (Olympus America, Center Valley, PA).

After 3 days of culture in CCM, the cells were transferred to osteogenic-inducing medium (bone differentiation medium, BDM) or adipogenic-inducing medium following a method reported previously for an additional 14 days.[22] The BDM is composed of CCM supplemented with 10 nM dexamethasone, 20 mM β-glycerolphosphate, and 50 μM L-ascorbic acid 2-phosphate. The adipogenic-inducing medium is composed of CCM supplemented with 0.5 μM dexamethasone, 0.5 μM isobutylmethylxanthine, and 50 μM indomethacin. Another set of samples was continuously cultured in CCM for the same period of time as the control. At day 7 and day 14 after induction began, samples were washed with PBS and collected for DNA analysis. At day 7 and day 14, the cells in osteogenic-induction culture were assayed to determine alkaline phosphatase (ALP) activity and calcium deposition following the previously published methods.[22] The calcium amount was by determined with ion coupled plasma (ICP) mass spectroscopy (Leeman Laboratories, Lowell, MA). Briefly, the samples were completely dissolved by 12 M HCl and diluted 10 times for ICP analysis. The calcium amount was normalized to DNA amount in order to diminish cell number difference. Von Kossa staining was also performed to visualize the mineralization of ECM. At the same time points, the cells in adipogenic-induction culture were stained with Nile red to detect lipid vacuoles. The data was pooled for statistical analysis; n = 3 for each sample.

Growth Factors Assay. An enzyme-linked immunosorbent assay (ELISA) was performed to quantify the amount of growth factors present in the cell culture environment. Growth factors embedded in the hMSC sheets were extracted as previously described.[23] Briefly, each tissue sheet from a 12-well plate was soaked in 1 mL of urea-heparin extraction buffer consisting of 2 M urea and 5 mg/mL heparin in 50 mM Tris with protease inhibitors [1 mM phenylmethylsulfonyl fluoride (PMSF), 5 mM benzamidine, and 10 mM *N*-ethylmaleimide (NEM)] at pH 7.4. The extraction mixture was rocked at 4 °C for 24 h and then centrifuged at 12 000*g* for 30 min at 4 °C, and the supernatants were collected. Osteogenesis related growth factors angiopoietin-1 (Ang1),

DOI: 10.1021/acsami.5b07386
ACS Appl. Mater. Interfaces 2015, 7, 23239−23247

Table 1. Primer Sequences Used for PCR

common name	gene ID	forward sequence	reverse sequence
GAPDH	GAPDH	5′-ACAGTTGCCATGTAGACC	5′-TTTTTGGTTGAGCACAGG
Sox-2	SOX2	5′-ATAATAACAATCATCGGCGG	5′-AAAAAGAGAGAGGCAAACTG
PPARG	PPARG	5′-TCATAATGCCATCAGGTTTG	5′ - CTGGTCGATATCACTGGAG
CEBPA	CEBPA	5′-AGCCTTGTACTGTATG	5′-AAAATGGTTTAGCAGAG
osteocalcin	BGLAP	5′-TTCTTTCCTCTTCCCCTTG	5′-CCTCTTCTGGAGTTTATTTGG
osteonectin	SPARC	5′-AGTATGTGTAACAGGAGGAC	5′-AATGTTGCTAGTGTGATTGG
OCT-4	POU5F1	5′ - GATCACCCTGGGATATACAC	5′ - GCTTTGCATATCTCCTGAAG
Rex-1	ZFP42	5′-GAATTCAGACCTAACCATCG	5′-TGAGCACTACTAGAGTGAAG

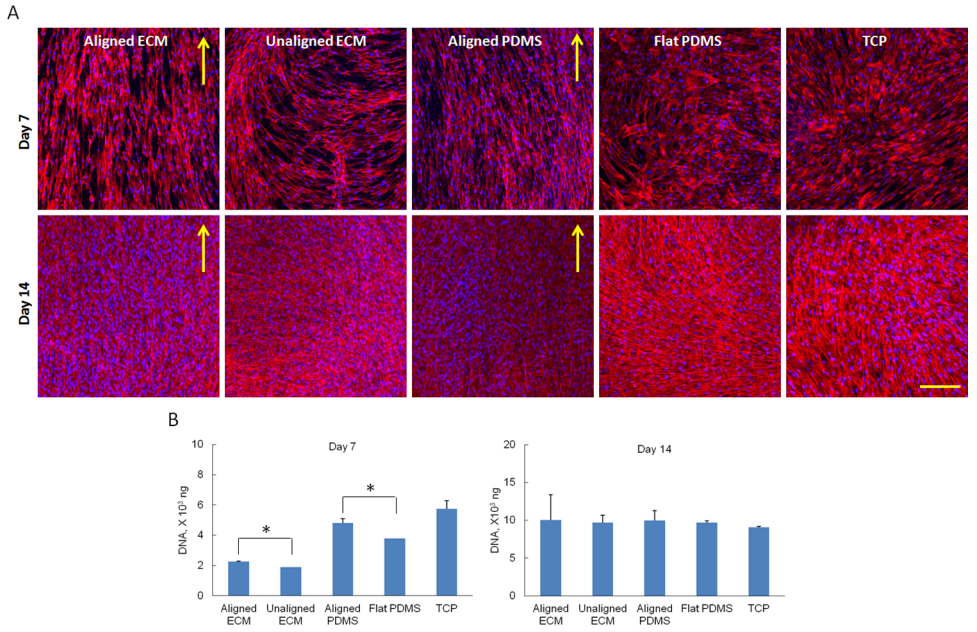

Figure 1. hMSC growth on different substrates. (A) Cell nucleus and F-actin staining. Arrows indicate cell alignment direction. Scale bar: 100 μm. (B) DNA quantification at day 7 and day 14. *$p < 0.05$. By day 14, the cell growth is comparable on all of the substrates.

transforming growth factor-β1 (TGF-β1), vascular endothelial growth factor (VEGF), and basic fibroblast growth factor (bFGF) were determined using ELISA kits (R&D Systems, Minneapolis, MN) according to the manufacturer's instruction. Values of optical density were measured spectrophotometrically (Molecular Devices, Sunnyvale, CA) at 450 nm and correction wavelength was set at 540 nm. In each experiment, three identical samples of each condition were examined and all samples and standards were measured in duplicate.

Scanning Electron Microscopy (SEM). The samples were prepared by incubation of different substrates (ECM, collagen I -coated PDMS, and TCP) in either CCM or BDM for 14 days. Then the samples were fixed in 4% paraformaldehyde, washed with PBS, and dehydrated through a graded series of ethanol. Finally the samples were dried in hexamethyldisilazane (Sigma), sputter-coated with a 5 nm platinum coating, and viewed using a Hitachi S-4700 field emission scanning electron microscope (Hitachi America, Troy, MI).

Reverse Transcription Polymerase Chain Reaction (RT-PCR). After 14 days of induction culture in differentiation medium, total RNA from different cultures were isolated using the Rneasy Mini kit (Qiagen, Valencia, CA). Reverse transcription (RT) was performed using 8 pg of total RNA with RT reaction mixture, which contains primers specific for target genes that were purchased from sigma and normalized to GAPDH as an endogenous control. RT-PCR reactions were performed on StepOnePlus RT-PCR system (Applied Biosystems, Foster City, CA), using SYBR1 Green PCR Master Mix. The amplification reactions were carried out for up to 35 cycles. Fold variation in gene expression was quantified using the comparative Ct method: $2^{(\mathrm{CtTreatment}-\mathrm{CtControl})}$. The primer sequences for target genes are listed in Table 1.

Statistics/Data Analysis. Experiment results were expressed as means ± standard deviation (SD) of the means of the samples. Student's *t* test (Microsoft Excel) was used for comparisons and statistical significance was accepted at $p < 0.05$.

RESULTS

Cell Proliferation on Different Substrates. The morphology of cells grown on different substrates was shown in Figure 1A. On day 7, cells on aligned ECM and aligned PDMS showed clear orientation; while cells on unaligned ECM, flat PDMS, and TCP showed random organization. On day 14, a high density of cells was observed on all substrates. The cells on aligned substrates still showed preferred orientation. Although some cells on unaligned substrates showed certain degree of alignment in local area, the overall orientation was not organized. The cell proliferation on different substrates was demonstrated in Figure 1B. On day 7, cell numbers on ECM (both aligned and unaligned) were much lower than those on PDMS (both aligned and flat) and TCP. In addition, cell numbers on aligned substrates (aligned ECM and aligned PDMS) was significantly higher than those on the corresponding unaligned substrates (unaligned ECM and flat PDMS). On day 14, the cell numbers on all substrates were comparable. The cell numbers on aligned ECM and PDMS were slightly higher than those on the corresponding unaligned substrates, but there was no significant difference.

DOI: 10.1021/acsami.5b07386
ACS Appl. Mater. Interfaces 2015, 7, 23239−23247

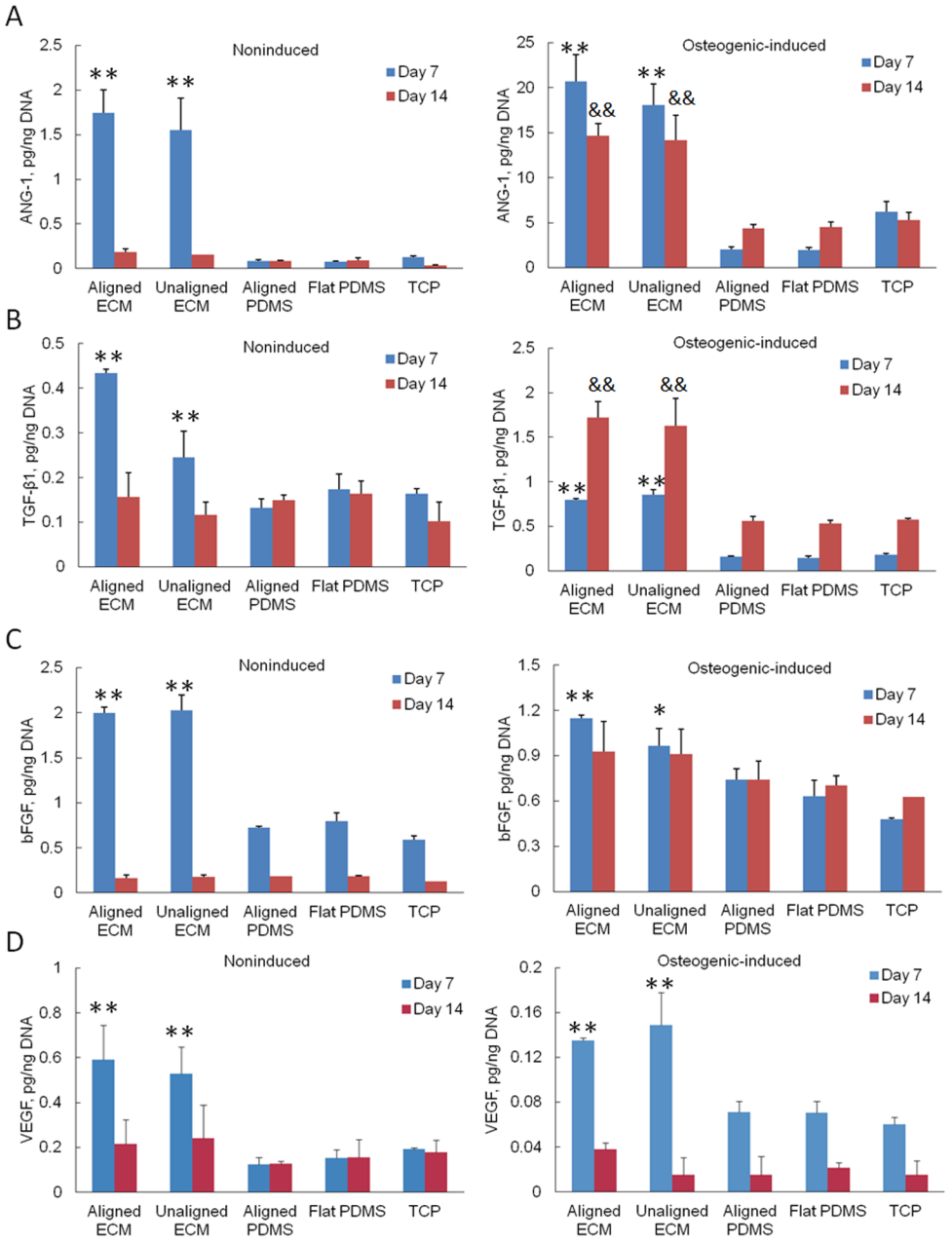

Figure 2. Quantification of different growth factors in both noninduced and osteogenic-induced culture on different substrates. (A) ANG-1; (B) TGF-β1; (C) bFGF; (D) VEGF. *$p < 0.05$, **$p < 0.01$ compared to PDMS and TCP on day 7; $^{\&\&}p < 0.01$ compared to PDMS and TCP on day 14. ECM samples contained the highest amount of growth factors.

Growth Factor Presence in the Microenvironment. The growth factors related to osteogenesis were quantified and shown in Figure 2. Overall speaking, the growth factors extracted from the ECM sheet were much higher than other substrates. For osteogenic-induced hMSCs, both the total and normalized ANG-1 amounts were much higher than those in the noninduced hMSC cultures (Figure 2A). Additionally, the ANG-1 level in ECM (both aligned and unaligned) cultures was around 10 times higher than that in PDMS (both aligned and flat) cultures and around 3 times higher than that in TCP cultures at day 7. The difference became smaller on day 14, which showed that the ANG-1 level in ECM culture was around 3 times higher than that in PDMS cultures. Comparing all the aligned and unaligned substrates, the ANG-1 level had no significant difference. For noninduced hMSCs, the ANG-1 level in the ECM (both aligned and unaligned) cultures was around 20 times higher than that in PDMS (both aligned and unaligned) cultures and around 13 times higher than that in TCP cultures. Despite the decrease on day 14, the ANG-1 amount in the ECM culture was still around twice higher than that in PDMS culture. In addition, the ANG-1 content in aligned substrates (aligned ECM and aligned PDMS) was higher than the corresponding unaligned substrates (unaligned ECM and PDMS) except PDMS on day 14; however, the difference was not significant.

The overall trend of TGF-β1 level was similar to that of ANG-1. The TGF-β1 amount in ECM cultures was significantly higher than that in PDMS and TCP cultures for both osteogenic-induced and noninduced hMSCs cultures (Figure 2B). Furthermore, all the induced cultures contained a much higher amount of TGF-β1 than the noninduced cultures. Similarly, the

DOI: 10.1021/acsami.5b07386
ACS Appl. Mater. Interfaces 2015, 7, 23239−23247

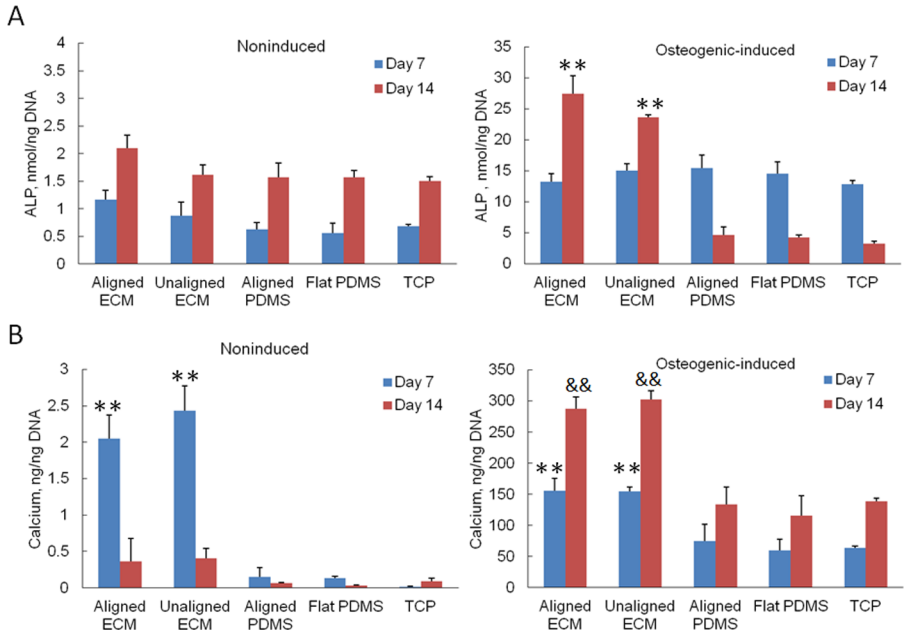

Figure 3. ALP activity (A) and calcium deposition (B) from hMSCs in both noninduced and osteogenic-induced cultures on different substrates. ** $p < 0.01$ compared to PDMS and TCP on day 7; $^{\&\&}p < 0.01$ compared to PDMS and TCP on day 14. ECM samples demonstrated the highest ALP activity and calcium deposition amount.

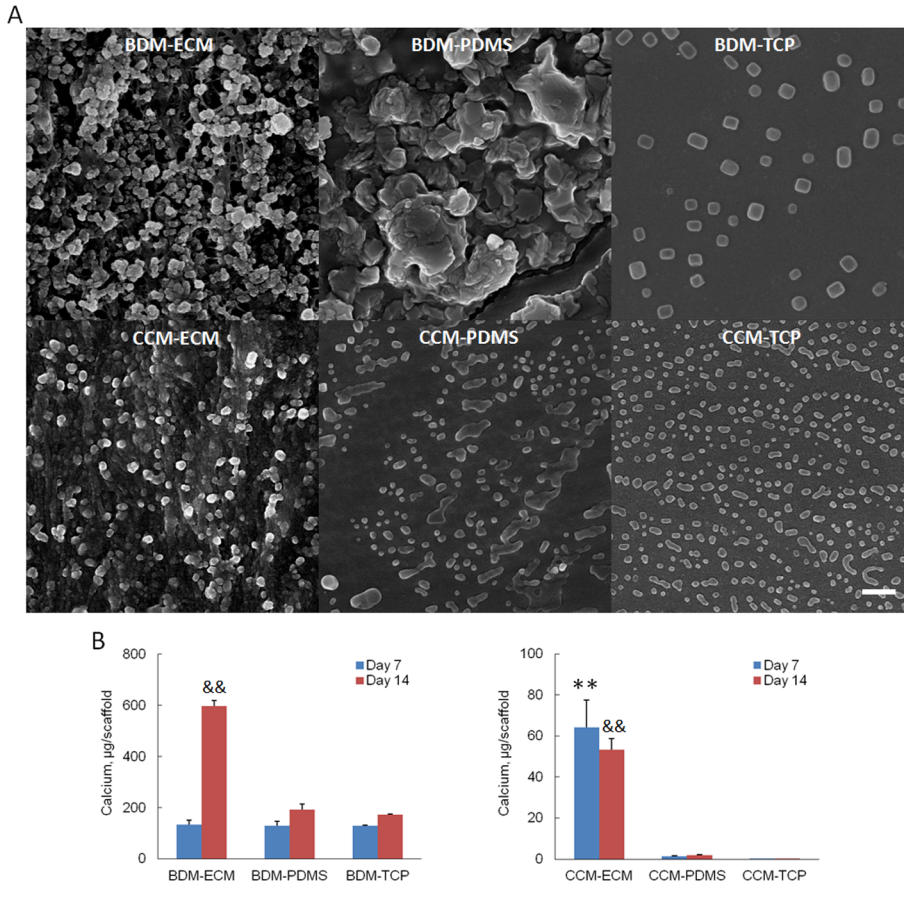

Figure 4. Calcium adsorption on different substrates (ECM, PDMS, and TCP) without cells in both osteogenic-induction medium (BDM) and complete cell medium (CCM). (A) Surface morphology of the substrates at day 14. Scale bar: 1 μm. (B) ICP quantification of calcium. **$p < 0.01$ compared to PDMS and TCP on day 7; $^{\&\&}p < 0.01$ compared to PDMS and TCP on day 14. There was much more calcium adsorbed on the ECM scaffold.

DOI: 10.1021/acsami.5b07386
ACS Appl. Mater. Interfaces 2015, 7, 23239−23247

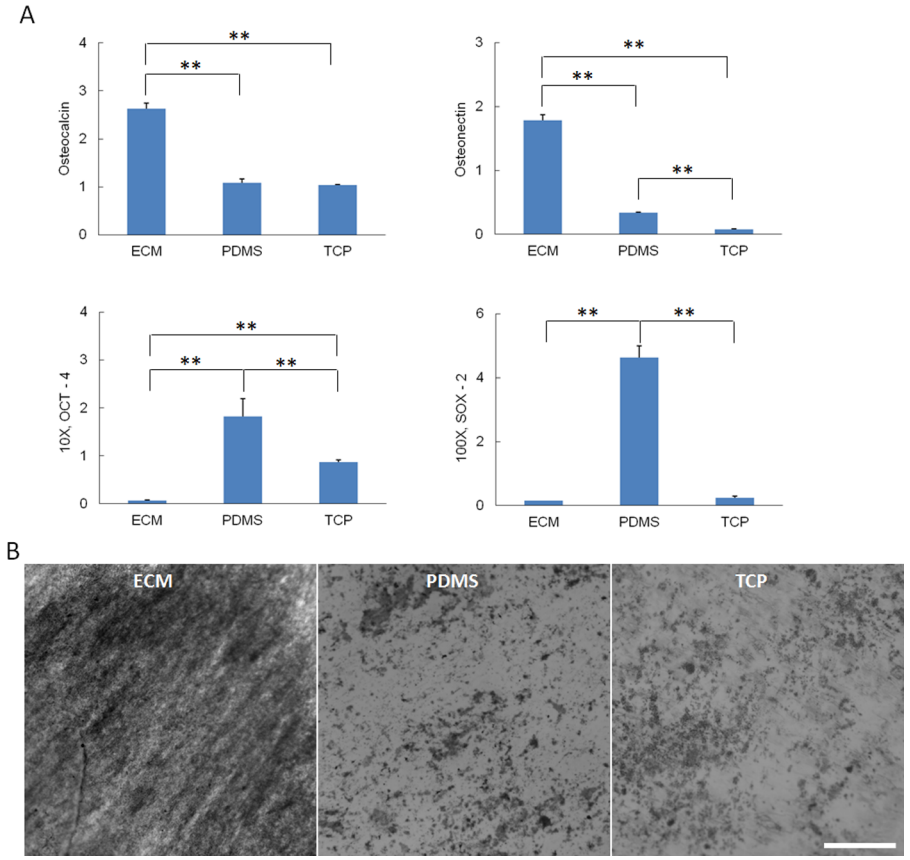

Figure 5. Gene expression (A) and Von Kossa staining (B) of osteogenic-induced hMSCs cultured on different substrates at day 14. $^{**}p < 0.01$. Scale bar: 100 μm. ECM samples showed significantly higher expression of osteogenesis-related genes and more mineralization.

b-FGF (Figure 2C) and VEGF (Figure 2D) levels in ECM cultures were significantly higher than those in PDMS and TCP cultures, for both osteogenic-induced and noninduced hMSC cultures. However, unlike the ANG-1 and TGF-β1, the induced cultures contained lower amounts of bFGF and VEGF compared to the corresponding noninduced cultures. Again, there was no significant difference between aligned and the corresponding unaligned samples. And among all the growth factors present in the induced culture, the ANG-1 level in ECM substrates was dramatically higher than the levels of TGF-β1, b-FGF, and VEGF.

ALP and Calcium Deposition of hMSCs. The ALP activity assay in Figure 3A demonstrated that on day 7 all samples exhibited comparable ALP expression. On day 14, the ALP level was much higher on ECM sheet than on other substrates. And the cells on aligned ECM showed significantly higher ALP activity than those on unaligned ECM. However, no significant difference was observed between aligned and flat PDMS samples. The ALP activity of undifferentiated hMSCs on different substrates was low, as expected. The cells on ECM (both aligned and unaligned) showed slightly higher ALP activity than the other samples.

Quantification of calcium deposition in both induced and noninduced cell cultures (Figure 3B) revealed that ECM cultures contained significantly higher calcium amount than those maintained on PDMS and TCP. However, still no significant difference was found between aligned and unaligned substrates in both induced and noninduced cultures. Overall, induced cultures contained approximately 100 times higher of calcium than noninduced cultures.

Calcium Adsorption on Different Substrates. According to the results from cell proliferation, growth factor analysis, ALP, and calcium quantification, the alignment of the substrates did not play a critical role in neither regulation of in vitro hMSCs growth nor osteogenic differentiation on these substrates. Therefore, the following experiments focused on comparison of substrates with different composition (ECM, collagen I-coated PDMS, and TCP). The substrates themselves can absorb calcium from the medium, which could be one of the reasons leading to enhanced osteogenic potential. Calcium adsorption on ECM, PDMS, and TCP without cells on day 14 was demonstrated in Figure 4. The under microsized particles were observed in both BDM and CCM culture (Figure 4A). These were possibly calcium phosphate (CaP) and protein crystals. Energy dispersive spectroscopy analysis revealed that calcium peaks in BDM samples were much stronger than CCM samples (data not shown). There were considerably more and finer CaP particles deposited on BDM-ECM than all other samples. The amount of CaP particles on BDM-PDMS appeared larger than on BDM-TCP. The CaP should be crystalline since amorphous CaP easily transforms into crystalline phase in aqueous medium.[24] The quantification of calcium adsorption in Figure 4B revealed that when incubated in induction medium (BDM), the three substrates adsorbed similar amount of calcium on day 7. While on day 14, ECM adsorbed around three times higher of calcium than PDMS and TCP. The calcium amount in BDM-ECM was significantly higher than that in CCM-ECM. From day 7 to day 14, the calcium amount increased around 4.5 times in BDM-ECM; whereas the calcium amount did not change significantly in CCM-ECM.

DOI: 10.1021/acsami.5b07386
ACS Appl. Mater. Interfaces 2015, 7, 23239−23247

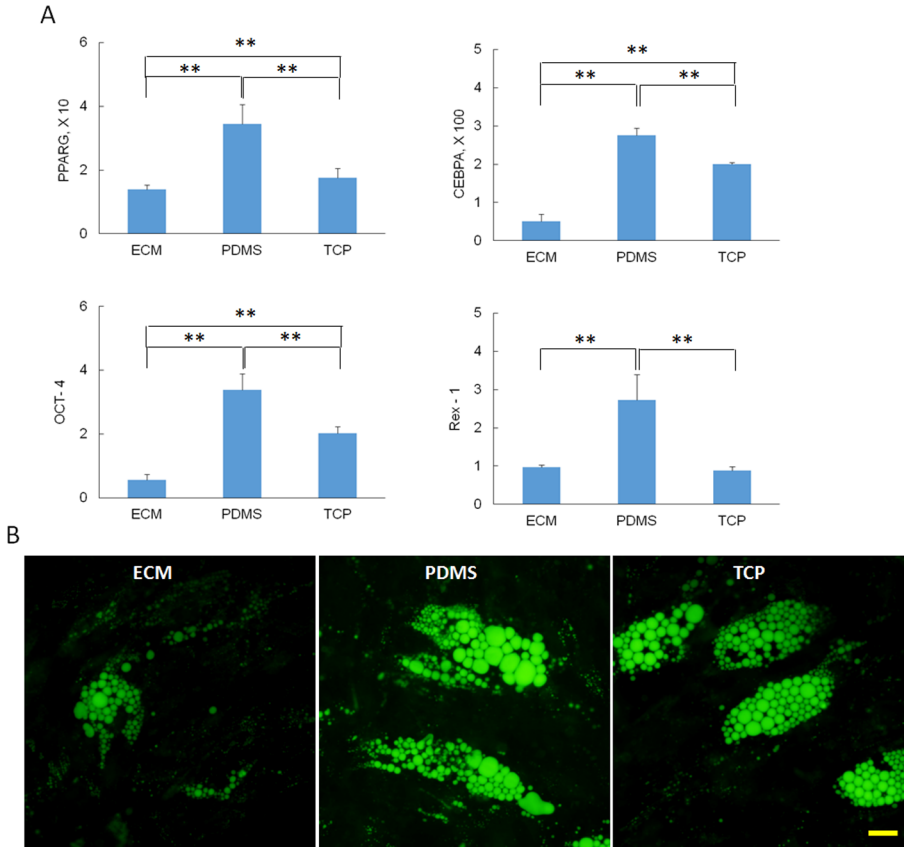

Figure 6. Gene expression (A) and Nile red staining (B) for adipogenic-induced hMSCs culture on different substrates at day 14. $^{**}p < 0.01$. Scale bar: 10 μm. ECM samples showed much lower expression of adipogenesis-related genes and fewer lipid vacuoles.

Osteogenic and Stemness Gene Expression. The expression of osteogenic and stemness-related genes (Figure 5A) from hMSCs cultured in osteogenic induction medium was normalized to endogenous gene (GAPDH) as well as to the corresponding control culture. Osteocalcin was significantly upregulated in ECM samples (approximately 2 times higher than PDMS and TCP samples). Osteonectin was highly expressed in ECM samples (approximately 5 times higher than PDMS samples and 22 times higher than TCP samples). Osteonectin expression in PDMS samples was also significantly higher than in TCP samples. OCT-4 and SOX-2 are frequently used as markers for undifferentiated stem cells. ECM samples had the lowest expression of these two markers, while PDMS samples maintained highest stemness marker expression. Von Kossa staining (Figure 5B) also showed more advanced osteogenesis in ECM samples with darker mineral deposition.

Adipogenic Differentiation. The expression of adipogenic and stemness-related genes (Figure 6A) from hMSCs cultured in adipogenic differentiation medium was normalized to endogenous gene (GAPDH) as well as to the corresponding control culture. Adipocyte-specific genes PPARG and CEBPA were upregulated in all cultures, but ECM samples had significantly lower increase than PDMS and TCP samples. The stemness markers OCT-4 and Rex-1 also demonstrated that the ECM samples had the lowest expression. The Nile red staining (Figure 6B) was correspondent with gene expression. The ECM samples had significantly less lipid vacuoles formation than PDMS and TCP samples.

DISCUSSION

A flexible cellular constructs with osteogenic and angiogenic potential can serve as periosteum to fit around bone graft of any size or shape for enhanced bone regeneration. The hMSC-seeded, fibroblast-derived ECM sheet could be a promising candidate for engineered periosteum. First, the ECM mimics the complex ECM microenvironment of native periosteum. It was found that collagen I and vitronectin were the two most important ECM molecules in promoting osteogenesis through $\alpha 1\beta 1$ and $\alpha v\beta 3$ integrin binding.[25] Second, there are many active binding sites in ECM sheet for entrapment of various growth factors and calcium. For example, ECM component heparin sulfate proteoglycans have specific binding for bFGF, fibronectin specifically binds TGF-β.[26,27] These growth factors play important roles in major signaling pathways responsible for osteogenesis.[28] Third, the ECM sheet can support the growth of MSCs, which have great osteogenic differentiation ability. The live osteogenic cells that are capable of producing new bone are the necessary components for engineered periosteum. Although the native periosteum showed anisotropic structure and mechanical properties,[29] the alignment of the substrates did not significantly influence the in vitro osteogenic differentiation of hMSCs and growth factor storage in our study.

Our fibroblast-derived ECM sheet culture showed lower cell numbers at day 7 compared to PDMS and TCP cultures (Figure 1B). This phenomenon was different from the results of other studies that found decorating stromal stem cell derived ECM on synthetic substrates can promote cell proliferation.[30] The lower cell proliferation in our study was probably caused by the different stiffness of the substrates. Previous studies also

DOI: 10.1021/acsami.5b07386
ACS Appl. Mater. Interfaces 2015, 7, 23239−23247

demonstrated that stiffer matrix could enhance endothelial cells and breast cancer cells proliferation.[31,32] The ECM sheet is around 35 μm thick and much softer than collagen I coated PDMS and TCP, which may lead to low cell growth rate at the beginning. However, the cell proliferation on ECM sheet kept up with other substrates by day 14, which may be attributed to the greater amount of growth factors in the ECM sheet promoting cell growth. Besides the influence on cell proliferation, the matrix stiffness also affected the differentiation of hMSCs. Rigid substrates tends to induce the osteogenic differentiation of MSCs.[33−35] However, in our study, the cells on softer substrates (ECM) sheet showed much higher ALP activity (Figure 3A) and calcium deposition (Figure 3B), which indicated that the environmental cues other than the rigidity of the substrates exerted larger influence on hMSCs. In addition to soluble chemical cues existing in the osteogenic induction medium, the growth factors present in the microenvironment also can regulate the differentiation of hMSCs. Generally speaking, ECM sheets can efficiently bind significantly higher amounts of growth factors than the other substrates. All of the four growth factors were involved in the two indispensable processes: angiogenesis and osteogenesis. ANG-1 is widely recognized as an angiogenic factor to promote microvessel stabilization.[36] ANG-1 was also reported to have a significant function in regulating osteogenesis. Osteoblasts overexpressing ANG-1 can enhance bone mass in vivo.[37] The immobilization of integrin-binding sequence of ANG-1 on titanium can significantly promote osteoblast differentiation, bone matrix deposition, and mineralization.[38] TGF-β1 was reported as a proangiogenic factor that improves EC migration and proliferation or vessel maturation.[39] TGF-β pathways are also one of the major signaling cascades responsible for osteogenesis. The disruption of TGF-β pathways can cause various bone disorders.[28] The osteogenic differentiation medium stimulated the hMSCs to secret around 10 times higher ANG-1 than those in normal cell culture medium (Figure 2A). The osteogenic-differentiated cultures also expressed higher levels of TGF-β1 than noninduced cultures (Figure 2B). The high local concentration of ANG-1 and TGF-β1 will benefit the bone generation. VEGF and bFGF are two of the most well-known angiogenic factors capable of stimulating new blood vessel formation.[40] bFGF is also an autocrine growth factor controlling in vitro bone formation.[41] Significant higher levels of bFGF in ECM samples (Figure 2C), in both induced and noninduced cultures, indicated that the microenvironment was more beneficial to stimulate bone cell replication. Due to the fact that angiogenesis and osteogenesis are closely correlated to bone growth, repair, and remodeling; significantly higher levels of VEGF in ECM samples would benefit osteogenesis in vivo (Figure 2D).

Calcium ion signaling pathway plays another important role in osteogenesis.[28] The increase of cytoplasmic Ca^{2+} led to increase of several growth factors which further signal cells for osteogenesis.[42] Thus, accumulation of calcium ions through CaP particle deposition can enhance osteoblastic activation and mineralization capacity of osteoprogenitor cells. Our ECM sheet clearly demonstrated significantly higher calcium accumulation capacity in both CCM and BDM (Figure 4B). Especially on day 14, the calcium content in BDM-ECM samples reached around 600 μg per scaffold, around three times higher than other substrates. Most of the ECM proteins are negatively charged including specific calcium-binding glycoproteins fibulins and thrombospondins, which facilitated the adsorption of Ca^{2+} from medium. The nanofibrous structure of ECM sheets also served as nucleation sites for CaP nanocrystal growth. The CaP-rich material is important in directing the phenotype of MSCs in bone tissue engineering applications.

The osteogenic gene expression profile further confirmed that hMSCs on an ECM sheet indeed had much higher osteogenic potential than the cells on other substrates, though the stemness significantly decreased (Figure 5A). Osteocalcin is a late stage bone marker genes, and osteonectin is a bone marker gene vital for calcium binding and bone mineralization. Both marker genes were significantly upregulated in ECM samples than other samples, which suggested that hMSCs cultured on ECM progressed more toward the osteogenesis path that the other cultures. This was also supported by decreased expression of stemness gene markers OCT-4 and SOX-2 that are critically involved in self-renewal of undifferentiated stem cells. However, the adipogenic potential of hMSCs on ECM scaffold was seriously inhibited (Figure 5B), which implied that the ECM microenvironment is more beneficial for osteogenic differentiation, but not for adipogenic induction. Taken together, the in vitro data suggest that it is reasonable to use osteogenic-differentiated hMSCs to construct periosteum on ECM sheet.

CONCLUSIONS

In summary, fibroblast-derived ECM sheets support hMSC growth and significantly influence hMSC differentiation, whereas the alignment of the substrate does not. The significantly higher amount of growth factors ANG-1, TGF-β1, bFGF, and VEGF in ECM sheets, as well as the accumulation of calcium phosphate on the ECM sheet surface, may be responsible for promoting the osteogenic differentiation of hMSCs. The adipogenic differentiation of hMSCs in ECM scaffolds was suppressed. The collagenous composition, nanofibrous structure, as well as osteogenesis-promoting microenvironment of fibroblast-derived ECM sheets would be beneficial for engineering artificial periosteum.

AUTHOR INFORMATION

Corresponding Author

*E-mail: fengzhao@mtu.edu. Tel: 906-487-2852. Fax: 906-487-1717.

Notes

The authors declare no competing financial interest.

ACKNOWLEDGMENTS

This study was supported by the National Institutes of Health (1R15HL115521-01A1) and the Research Excellence Fund-Research Seed Grant (REF-RS) from Michigan Technological University to F.Z.

REFERENCES

(1) Zhang, X. P.; Awad, H. A.; O'Keefe, R. J.; Guldberg, R. E.; Schwarz, E. M. A Perspective: Engineering Periosteum for Structural Bone Graft Healing. *Clin. Orthop. Relat. Res.* **2008**, *466* (8), 1777−1787.

(2) Dwek, J. R. The Periosteum: What Is It, Where Is It, and What Mimics It in Its Absence? *Skeletal Radiol.* **2010**, *39* (4), 319−323.

(3) Zhang, X. P.; Xie, C.; Lin, A. S. P.; Ito, H.; Awad, H.; Lieberman, J. R.; Rubery, P. T.; Schwarz, E. M.; O'Keefe, R. J.; Guldberg, R. E. Periosteal Progenitor Cell Fate in Segmental Cortical Bone Graft Transplantations: Implications for Functional Tissue Engineering. *J. Bone Miner. Res.* **2005**, *20* (12), 2124−2137.

(4) Squier, C. A.; Ghoneim, S.; Kremenak, C. R. Ultrastructure of the Periosteum from Membrane Bone. *J. Anat.* **1990**, *171*, 233−239.

(5) Fan, W.; Crawford, R.; Xiao, Y. Enhancing in Vivo Vascularized Bone Formation by Cobalt Chloride-Treated Bone Marrow Stromal Cells in a Tissue Engineered Periosteum Model. *Biomaterials* **2010**, *31* (13), 3580−3589.

DOI: 10.1021/acsami.5b07386
ACS Appl. Mater. Interfaces 2015, 7, 23239−23247

(6) Foolen, J.; van Donkelaar, C. C.; Nowlan, N.; Murphy, P.; Huiskes, R.; Ito, K. Collagen Orientation in Periosteum and Perichondrium Is Aligned with Preferential Directions of Tissue Growth. *J. Orthop. Res.* **2008**, *26* (9), 1263−1268.
(7) Xing, Q.; Vogt, C.; Leong, K. W.; Zhao, F. Highly Aligned Nanofibrous Scaffold Derived from Decellularized Human Fibroblasts. *Adv. Funct. Mater.* **2014**, *24* (20), 3027−3035.
(8) Weiner, S.; Wagner, H. D. The Material Bone: Structure Mechanical Function Relations. *Annu. Rev. Mater. Sci.* **1998**, *28*, 271−298.
(9) Chen, K.; Lin, X. F.; Zhang, Q.; Ni, J. H.; Li, J. M.; Xiao, J.; Wang, Y.; Ye, Y. H.; Chen, L.; Jin, K. K.; Chen, L. Decellularized Periosteum as a Potential Biologic Scaffold for Bone Tissue Engineering. *Acta Biomater.* **2015**, *19*, 46−55.
(10) Decaris, M. L.; Binder, B. Y.; Soicher, M. A.; Bhat, A.; Leach, J. K. Cell-Derived Matrix Coatings for Polymeric Scaffolds. *Tissue Eng., Part A* **2012**, *18* (19−20), 2148−2157.
(11) Datta, N.; Pham, Q. P.; Sharma, U.; Sikavitsas, V. I.; Jansen, J. A.; Mikos, A. G. In Vitro Generated Extracellular Matrix and Fluid Shear Stress Synergistically Enhance 3d Osteoblastic Differentiation. *Proc. Natl. Acad. Sci. U. S. A.* **2006**, *103* (8), 2488−2493.
(12) Sadr, N.; Pippenger, B. E.; Scherberich, A.; Wendt, D.; Mantero, S.; Martin, I.; Papadimitropoulos, A. Enhancing the Biological Performance of Synthetic Polymeric Materials by Decoration with Engineered, Decellularized Extracellular Matrix. *Biomaterials* **2012**, *33* (20), 5085−5093.
(13) Bae, S. E.; Bhang, S. H.; Kim, B. S.; Park, K. Self-Assembled Extracellular Macromolecular Matrices and Their Different Osteogenic Potential with Preosteoblasts and Rat Bone Marrow Mesenchymal Stromal Cells. *Biomacromolecules* **2012**, *13* (9), 2811−2820.
(14) Kang, Y. Q.; Kim, S.; Bishop, J.; Khademhosseini, A.; Yang, Y. Z. The Osteogenic Differentiation of Human Bone Marrow Mscs on Huvec-Derived Ecm and Beta-Tcp Scaffold. *Biomaterials* **2012**, *33* (29), 6998−7007.
(15) Caplan, A. I. Adult Mesenchymal Stem Cells for Tissue Engineering Versus Regenerative Medicine. *J. Cell. Physiol.* **2007**, *213* (2), 341−347.
(16) Caplan, A. I.; Dennis, J. E. Mesenchymal Stem Cells as Trophic Mediators. *J. Cell. Biochem.* **2006**, *98* (5), 1076−1084.
(17) Ghannam, S.; Bouffi, C.; Djouad, F.; Jorgensen, C.; Noel, D. Immunosuppression by Mesenchymal Stem Cells: Mechanisms and Clinical Applications. *Stem Cell Res. Ther.* **2010**, *1*, 2.
(18) Kang, Y.; Ren, L.; Yang, Y. Engineering Vascularized Bone Grafts by Integrating a Biomimetic Periosteum and Beta-Tcp Scaffold. *ACS Appl. Mater. Interfaces* **2014**, *6* (12), 9622−9633.
(19) Hoffman, M. D.; Benoit, D. S. W. Emulating Native Periosteum Cell Population and Subsequent Paracrine Factor Production to Promote Tissue Engineered Periosteum-Mediated Allograft Healing. *Biomaterials* **2015**, *52*, 426−440.
(20) Zhao, L.; Zhao, J.; Wang, S.; Wang, J.; Liu, J. Comparative Study between Tissue-Engineered Periosteum and Structural Allograft in Rabbit Critical-Sized Radial Defect Model. *J. Biomed. Mater. Res., Part B* **2011**, *97B* (1), 1−9.
(21) Zhao, F.; Veldhuis, J. J.; Duan, Y. J.; Yang, Y.; Christoforou, N.; Ma, T.; Leong, K. W. Low Oxygen Tension and Synthetic Nanogratings Improve the Uniformity and Stemness of Human Mesenchymal Stem Cell Layer. *Mol. Ther.* **2010**, *18* (5), 1010−1018.
(22) Zhao, F.; Grayson, W. L.; Ma, T.; Bunnell, B.; Lu, W. W. Effects of Hydroxyapatite in 3-D Chitosan-Gelatin Polymer Network on Human Mesenchymal Stem Cell Construct Development. *Biomaterials* **2006**, *27* (9), 1859−1867.
(23) Reing, J. E.; Brown, B. N.; Daly, K. A.; Freund, J. M.; Gilbert, T. W.; Hsiong, S. X.; Huber, A.; Kullas, K. E.; Tottey, S.; Wolf, M. T.; Badylak, S. F. The Effects of Processing Methods Upon Mechanical and Biologic Properties of Porcine Dermal Extracellular Matrix Scaffolds. *Biomaterials* **2010**, *31* (33), 8626−8633.
(24) Zhao, J.; Liu, Y.; Sun, W.-b.; Zhang, H. Amorphous Calcium Phosphate and Its Application in Dentistry. *Chem. Cent. J.* **2011**, *5*, 40−40.
(25) Salasznyk, R. M.; Williams, W. A.; Boskey, A.; Batorsky, A.; Plopper, G. E. Adhesion to Vitronectin and Collagen I Promotes Osteogenic Differentiation of Human Mesenchymal Stem Cells. *J. Biomed. Biotechnol.* **2004**, *2004*, 24−34.
(26) Lu, Q. Q.; Li, M. M.; Zou, Y.; Cao, T. Delivery of Basic Fibroblast Growth Factors from Heparinized Decellularized Adipose Tissue Stimulates Potent De Novo Adipogenesis. *J. Controlled Release* **2014**, *174*, 43−50.
(27) Hayashi, H.; Sakai, T. Biological Significance of Local Tgf-Beta Activation in Liver Diseases. *Front. Physiol.* **2012**, DOI: 10.3389/fphys.2012.00012.
(28) Hayrapetyan, A.; Jansen, J. A.; van den Beucken, J. Signaling Pathways Involved in Osteogenesis and Their Application for Bone Regenerative Medicine. *Tissue Eng., Part B* **2015**, *21* (1), 75−87.
(29) McBride, S. H.; Evans, S. F.; Tate, M. L. K. Anisotropic Mechanical Properties of Ovine Femoral Periosteum and the Effects of Cryopreservation. *J. Biomech.* **2011**, *44* (10), 1954−1959.
(30) Antebi, B.; Zhang, Z.; Wang, Y.; Lu, Z.; Chen, X. D.; Ling, J. Stromal-Cell-Derived Extracellular Matrix Promotes the Proliferation and Retains the Osteogenic Differentiation Capacity of Mesenchymal Stem Cells on Three-Dimensional Scaffolds. *Tissue Eng., Part C* **2015**, *21*, 171.
(31) Yeh, Y. T.; Hur, S. S.; Chang, J.; Wang, K. C.; Chiu, J. J.; Li, Y. S.; Chien, S. Matrix Stiffness Regulates Endothelial Cell Proliferation through Septin 9. *PLoS One* **2012**, *7* (10), e46889.
(32) Chen, L.; Zhang, Z.; Qiu, J.; Zhang, L.; Luo, X.; Jang, J. Chaperonin Cct-Mediated Aib1 Folding Promotes the Growth of Erα-Positive Breast Cancer Cells on Hard Substrates. *PLoS One* **2014**, *9* (5), e96085.
(33) Chen, J. C.; Jacobs, C. R. Mechanically Induced Osteogenic Lineage Commitment of Stem Cells. *Stem Cell Res. Ther.* **2013**, *4*, 107.
(34) Lee, J.; Abdeen, A. A.; Huang, T. H.; Kilian, K. A. Controlling Cell Geometry on Substrates of Variable Stiffness Can Tune the Degree of Osteogenesis in Human Mesenchymal Stem Cells. *J. Mech. Behav. Biomed. Mater.* **2014**, *38*, 209−218.
(35) Witkowska-Zimny, M.; Walenko, K.; Wrobel, E.; Mrowka, P.; Mikulska, A.; Przybylski, J. Effect of Substrate Stiffness on the Osteogenic Differentiation of Bone Marrow Stem Cells and Bone-Derived Cells. *Cell Biol. Int.* **2013**, *37* (6), 608−616.
(36) Yancopoulos, G. D.; Davis, S.; Gale, N. W.; Rudge, J. S.; Wiegand, S. J.; Holash, J. Vascular-Specific Growth Factors and Blood Vessel Formation. *Nature* **2000**, *407* (6801), 242−248.
(37) Suzuki, T.; Miyamoto, T.; Fujita, N.; Ninomiya, K.; Iwasaki, R.; Toyama, Y.; Suda, T. Osteoblast-Specific Angiopoietin 1 Overexpression Increases Bone Mass. *Biochem. Biophys. Res. Commun.* **2007**, *362* (4), 1019−1025.
(38) Feric, N. T.; Cheng, C. C. H.; Goh, M. C.; Dudnyk, V.; Di Tizio, V.; Radisic, M. Angiopoietin-1 Peptide Qhredgs Promotes Osteoblast Differentiation, Bone Matrix Deposition and Mineralization on Biomedical Materials. *Biomater. Sci.* **2014**, *2* (10), 1384−1398.
(39) Goumans, M. J.; Valdimarsdottir, G.; Itoh, S.; Rosendahl, A.; Sideras, P.; ten Dijke, P. Balancing the Activation State of the Endothelium Via Two Distinct Tgf-Beta Type I Receptors. *EMBO J.* **2002**, *21* (7), 1743−1753.
(40) Zisch, A. H.; Lutolf, M. P.; Hubbell, J. A. Biopolymeric Delivery Matrices for Angiogenic Growth Factors. *Cardiovasc. Pathol.* **2003**, *12* (6), 295−310.
(41) Bodo, M.; Lilli, C.; Bellucci, C.; Carinci, P.; Calvitti, M.; Pezzetti, F.; Stabellini, G.; Bellocchio, S.; Balducci, C.; Carinci, F.; Baroni, T. Basic Fibroblast Growth Factor Autocrine Loop Controls Human Osteosarcoma Phenotyping and Differentiation. *Mol. Med.* **2002**, *8* (7), 393−404.
(42) Liedert, A.; Kaspar, D.; Blakytny, R.; Claes, L.; Ignatius, A. Signal Transduction Pathways Involved in Mechanotransduction in Bone Cells. *Biochem. Biophys. Res. Commun.* **2006**, *349* (1), 1−5.

DOI: 10.1021/acsami.5b07386
ACS Appl. Mater. Interfaces 2015, 7, 23239−23247